Cascade Motion Planning for Vibration Suppression of the Focus Cabin in FAST

Zheng Rongzhang[1, 2], Jing Fengshui[2], Yang Guodong[2]

1. University of Chinese Academy of Sciences, Beijing 100190
E-mail:zhengrongzhang2015@ia.ac.cn

2. The State Key Laboratory of Management and Control for Complex Systems,
Institute of Automation, Chinese Academy of Sciences, Beijing 100190
E-mail:{fengshui.jing, guodong.yang}@ia.ac.cn

Abstract: The Five-hundred-meter Aperture Spherical Radio Telescope (FAST) requires high accuracy of positioning and attitude adjusting. Due to its flexible structure, the cable-cabin system can be excited to vibrate, which affects the performance. To alleviate the vibration during the slewing task, taking advantage of s-curve planning and input shaping, a cascade motion planning method is proposed. Considering the main vibration mode, a simplified cable-cabin model is built for simulation according to the parameters of FAST. Simulation experiments are conducted to prove that the cascade method is effective in vibration suppression and robust to the change of natural frequency.

Key Words: FAST telescope, vibration suppression, motion planning, s-curve, input shaping

1 Introduction

Located in Pingtang County of Guizhou Province in China, the Five-hundred-meter Aperture Spherical Radio Telescope (FAST) has been the largest single dish radio telescope in the world since completed in September, 2016. After fine tuning in the following three to five years, it will be able to detect radio from the deep universe with very high accuracy. Serving as a multi-science platform, the telescope will provide treasures to astronomers, as well as bring prosperity to other research [1].

Fig .1: The overview of FAST telescope

During the early design of FAST telescope, National Astronomical Observatories in Chinese Academy of Science, Tsinghua University and Xidian University did much research related to the structure, model and control. The final design is shown in Fig. 1. FAST adopted a novel design to detect signals with high accuracy by combining the active main reflector, cable-cabin system and Stewart platform together. Supported by six towers around, the 30-ton focus cabin is driven by six cables to reach the expected pose with a rough accuracy. Then the A-B rotator and Stewart platform (with the receivers mounted on its lower platform) serve as the secondary adjustable system to compensate the deviation of position and angle. The focus cabin and Stewart platform are shown in Fig. 2.

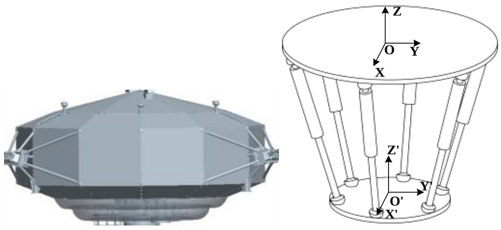

Fig. 2: The focus cabin and Stewart platform

Due to its flexible structure, FAST costs less and has a larger workspace than the Arecibo telescope, but it suffers nonlinearity, strong coupling and large lag, which pose a threat to controlling the system with high accuracy. What's more, flexibility is liable to introduce vibration, which would delay the settling time of the system operation, lower the accuracy and even damage the mechanical structure. Thus, vibration suppression becomes valuable and requires more attention and effort.

The vibration is mainly caused by three factors: random wind disturbance, excitation by motion of some parts of the structure and the counteraction of Stewart platform. Some methods were proposed to alleviate the vibration. S. Deng et al. planned the trajectory of On-The-Fly Observing for the feed receiver with double S velocity profile to smooth the motion [2]. J.H. Sun et al. designed novel reaction mass dampers according to the FAST structure [3], Y.X. Su et al. used electrorheological damper and adjusted the voltage with measured real-time wind speed to suppress vibration [4, 5]. Z.Q. Dong [6] and Q. Wei [7] proposed MTMD damper and a cable mass control scheme respectively. B. Zi et al. applied fuzzy immune PID controller to vibration suppression during the tracking [8]. Most of the published

*This work is supported by National Natural Science Foundation (NNSF) of China under Grant No. 61573358, and National Key Technology Support Program under Grant No. 2015BAF01B01.

research mainly focused on the design of physical dampers, which would change the system structure and take much cost.

Vibration suppression methods can roughly be classified into three categories: hardware design, feedback control and motion planning. Among them, input shaping is a kind of motion planning method which needs no extra devices to change system structure. In particular, it suits for systems whose key parameters are given as a priori [9]. First summarized by O.J.M Smith in the late 1950s [10], input shaping had been developed during the following decades and many extended forms emerged, such as ZV, ZVD, EI, SI and other kinds of shapers [11, 12, 13]. Because no researchers applied input shaping methods to vibration suppression of the focus cabin of FAST to date, it is meaningful to incorporate these methods into the control of FAST. In this paper, a cascade trajectory planning method, which utilizes the advantages of s-curve and input shaping, is proposed to suppress the vibration during the slewing task.

The rest of this paper is organized as follows. Section 2 describes the modelling of the cable-cabin system and given related parameters. Section 3 proposes the cascade trajectory planning method and demonstrates the design details in the process of introducing the background of s-curve planning and input shaping. Simulation experiments are carried out to prove the effectiveness of the proposed method in Section 4. Finally in Section 5, conclusion of the paper is drawn and some future improvements are raised out.

2 Problem Description and Modelling

As mentioned before, to satisfy the performance indices, the FAST feed support system adopts a two-level adjustment. When given the expected pose, the cable-driven system and the A-B rotator reach the assigned location and orientation roughly, which ensures the position error under 48mm and the angle error under 1 deg. According to the error measured, the change of Stewart platform's six legs are calculated and used to drive the lower platform to compensate the rough error. After two levels of adjustment, position and attitude accuracy will achieve the expected performance indices.

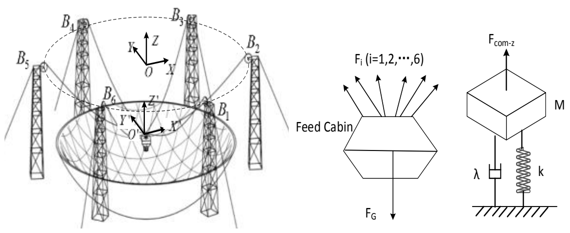

Fig. 3: Cable-cabin system and the equivalent model

To research the vibration suppression, a simple model is built first. Fig. 3 shows that the main forces acting on the focus cabin are pulls from the six cables and the gravity. The force and torque equations are

$$\begin{cases} \sum_{i=1}^{6} \mathrm{F_i} + \mathrm{F_G} = \mathrm{F_{com}} \\ \sum_{i=1}^{6} r_i \times F_i + \tau_G = \tau_{com} \end{cases} \tag{1}$$

where the variables are all vectors, $\mathrm{F_{com}}$ is the composition of forces, τ_{com} is the composition of torques, r_i is the vector pointing from the reference point for torque calculating to the mounting point connecting the i$^{\text{th}}$ cable and the cabin, τ_G is the gravitation torque.

Because of the influence of mass and flexibility of cables, it is difficult to model the real cable-cabin structure precisely and a complex model often leads to trouble. So it is necessary to simplify the problem. Actually the maximum angular velocity of the A-B rotator is 1.2×10^{-3} rad/s, which can hardly contribute to the vibration, so the A-B rotator is neglected. Moreover, the focus cabin's torsional vibration is not considered because it relates to its pose, which makes the model more complicated. The algorithm proposed is aimed at parallel vibration suppression. A formal simulation report [14] came out with the joint efforts of Chinese and German technicians. They used Finite Element Analysis to get the cable-cabin model and the range of natural frequencies, among which the first order resonant frequency is the most significant. The spring and damper model is chosen to get the first order vibrating model. The composition of force $\mathrm{F_{com}}$ can be decomposed into three force along the axes of Cartesian coordinate, $\mathrm{F_{com-x}}$, $\mathrm{F_{com-y}}$ and $\mathrm{F_{com-z}}$. Meanwhile the spring and damper model is used to describe vibration along every axis, as Fig. 3 shows. Along the z axis, the following differential equation is established.

$$M\ddot{l} = \mathrm{F_{com-z}} - k(l - l_0) - \lambda\dot{l} \tag{2}$$

Arrange it to be more simplified,

$$\ddot{l} + \frac{\lambda}{M}\dot{l} + \frac{k}{M}l = \frac{\mathrm{F_{com-z}}}{M} + \frac{k}{M}l_0 \tag{3}$$

where l is the displacement along the z axis, k is the spring constant, λ is the damper constant, l_0 is the offset of the spring. To derive the formula relating the damping ratio and natural frequency to the spring and damper constant, let $\frac{\mathrm{F_{com-z}}}{M} + \frac{k}{M}l_0 = 0$, then

$$\ddot{l} + 2\xi\omega_n\dot{l} + \omega_n^2 l = 0 \tag{4}$$

By comparing formula (3) with (4),

$$\begin{cases} 2\xi\omega_n = \frac{\lambda}{M} \\ \omega_n^2 = \frac{k}{M} \end{cases} \tag{5}$$

According to the aforementioned report, the first order resonant frequency is between 0.18 to 0.22 Hz, the second order resonant frequencies are above 0.28Hz, so in the model, the natural frequency is chosen to be $f_n = 0.18Hz$, and $\omega_n = 2\pi f_n$. The cables' damping ratios are usually very small and it is estimated to be $\xi = 0.2\%$ [3]. When using modules to build the model, the spring and damper constant k and λ should be assigned properly. They can be derived from formula (5).

$$\begin{cases} \mathrm{k} = M\omega_n^2 = M(2\pi f_n)^2 \\ \lambda = 2\xi\omega_n M \end{cases} \tag{6}$$

Some important parameters and performance indices are listed in Table 1 for reference.

Table 1: Related Parameters and Performance Indices

Positioning accuracy of the cable-driven system	±48 mm
Maximum velocity of the focus cabin	400 mm/s
Positioning accuracy of the A-B rotator	$\pm 1^{\circ}$
Maximum rotational speed of the A-B rotator	1.2×10^{-3} rad/s
Maximum rotational acceleration of the A-B rotator	4×10^{-5} rad/s^2
Natural frequency of the cable-cabin system (f_n)	0.18Hz
Damping ratio of the cable-cabin system (ξ)	0.2%
Mass of the focus cabin (M)	3×10^4 kg
Local gravitational constant (g)	9.81N/kg
Spring constant (k)	3.8334×10^4 N/m
Damper constant (λ)	43.2 N s/m
Sampling rate	5 Hz

3 Cascade Trajectory Planning for Vibration Suppression

To meet the requirement of rapidity, engineers tend to make the system driven as fast as possible. However, quick start and stop can excite the vibration of flexible structure like the cable-cabin system discussed. Since the damping ratio is very small, the cable-cabin system will vibrate for a long time once excited. The vibration of the 30-ton focus cabin not only reduces positioning accuracy and prolongs the settling time, but also shorten the lifespan of mechanical components and even damage some part of the structure. If the system operates without motion planning in the slewing task (move from the assigned start point to the end point), the vibration is shown in Fig. 4. In Fig. 4 (a), the deviation of the real position from the plan is expected to be zero at t=40s, but the vibration grows stronger for quick stop and goes far beyond 48mm. Fig. 4 (b) shows that in the frequency domain, the main vibration energy is focused near 0.18Hz.

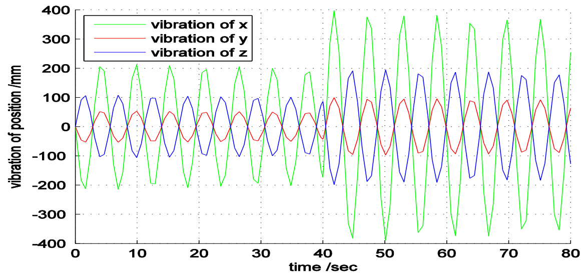

(a)

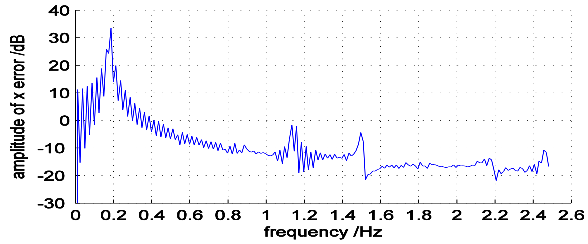

(b)

Fig. 4: Vibration in time and frequency domains without motion planning

To alleviate the vibration during the slewing task, the cascade trajectory planning method is proposed. The diagrams in Fig 5. illustrate the whole procedure of the slewing task. First observation parameters are given to feed Cascade Trajectory Planning, then the output is decomposed by Position & Attitude Assignment into control signals, and finally Actuators are driven to complete the task. The cascade trajectory planning module consists of 2 sub modules, s-curve planning and input shaping. The s-curve planning is used to suppress vibration of a wide spectrum of frequency and partly optimized for the natural frequency. The input shaping focus on vibration suppression near the natural frequency, because the s-curve planning cannot eliminate vibration near the natural frequency totally. The following subsections will discuss them in detail.

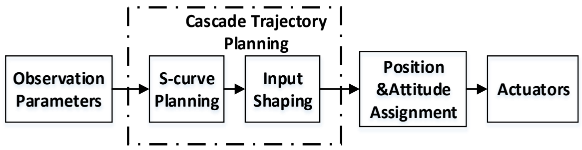

Fig. 5: Procedure of the slewing task

3.1 S-curve Planning

Generally speaking, proper motion planning keeps balance between rapidity and stability and at the same time suppresses vibration. The planned position, velocity, acceleration and jerk profiles of s-curve planning are depicted in Fig. 6. C. Lewin [15] compared the trapezoidal motion profile with s-curve and made a conclusion that the trapezoidal motion profiles excite more vibration in a wide range of spectrum than s-curve does, for the reason that its acceleration profile is not continuous. Peter H. Meckl et al. [16] optimized the ramp-up time of s-curve to achieve fast motion with minimum vibration and the method is most pronounced for systems having low natural frequencies and requiring fast motions. So the optimized s-curve planning is adopted in the cascade trajectory planning method.

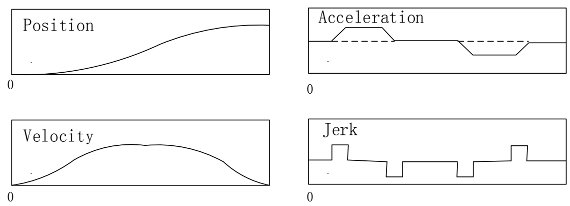

Fig. 6: S-curve planning

Given the maximum limits of velocity (400 mm/s), acceleration (80 mm/ s^2) and jerk (50 mm/ s^3), parameters of the profile are calculated according to Meckl's method. The key parameter $\omega_n t_r/2\pi = 0.9$, with which the optimal ratio of ramp-up time to the accelerating time is found to be $t_a^* = 0.5$. Then the ramp-up time of the acceleration comes out with 5.0s and the total time of acceleration is 10.0s. The rest of the s-curve profile is planned as usual.

3.2 Input Shaping

In this subsection, the foundation of input shaping is laid first and then combination of the shapers and our model is discussed. The basic procedure of input shaping is to convolve several impulses of various amplitudes and time delays with the original input command, then the shaped command is used as an alternative to the original. Fig. 7 is a simple demonstration. Fig. 7 (a) shows the responses of impulse P1 and P2 respectively. If their amplitudes and time delays are chosen properly, the two impulses result in no vibration. Fig. 7 (b) illustrates how to get the shaped command.

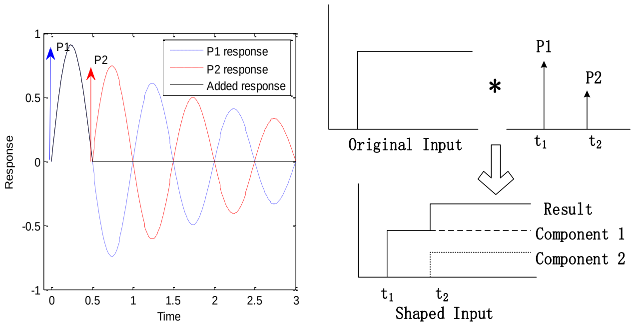

Fig. 7: Basic idea of input shaping, (a) the self-canceling result of a two-impulse shaper, (b) convolve the reference input with the shaper

Usually a shaper consists of n impulses whose amplitudes are A_i and time delays are t_i (i=1, 2, … , n). An optimization problem is solved to get the impulses' parameters, with the constraint that the amplitude of vibration equals to zero at the natural frequency. For the Zero Vibration (ZV) shaper, the two impulses is

$$\begin{bmatrix} A_i \\ t_i \end{bmatrix} = \begin{bmatrix} \frac{1}{1+K} & \frac{K}{1+K} \\ 0 & \frac{\pi}{\omega\sqrt{1-\xi^2}} \end{bmatrix} \quad (7)$$

where

$$\mathrm{K} = e^{\left(\frac{-\xi\pi}{\sqrt{1-\xi^2}}\right)}$$

As discussed in Section 2, the natural frequency and damping ratio of the model is 0.18Hz and 0.2%, so $\omega = 2\pi f_n = 2\pi \times 0.18\ \mathrm{rad/s} = 1.13\ \mathrm{rad/s}$ and $\xi = 0.002$, the two-impulse shaper is

$$\begin{bmatrix} A_i \\ t_i \end{bmatrix} = \begin{bmatrix} 0.5016 & 0.4984 \\ 0 & 2.7802 \end{bmatrix}$$

Actually, because of modelling error, the estimated natural frequency and damping ratio are not exactly equal to the real ones. As Fig. 8 shows, ZV shaper is sensitive to modelling error. To make the shaper more robust to the natural frequency, another constraint is added.

$$\frac{\partial}{\partial\omega}\mathrm{V}(\omega,\xi) = 0 \quad (8)$$

The solution is

$$\begin{bmatrix} A_i \\ t_i \end{bmatrix} = \begin{bmatrix} \frac{1}{K^2+2K+1} & \frac{2K}{K^2+2K+1} & \frac{K^2}{K^2+2K+1} \\ 0 & \frac{\pi}{\omega\sqrt{1-\xi^2}} & \frac{2\pi}{\omega\sqrt{1-\xi^2}} \end{bmatrix} \quad (9)$$

This three-impulse shaper is called the Zero Vibration and Derivative (ZVD) shaper. Again combined with our model, the ZVD shaper is

$$\begin{bmatrix} A_i \\ t_i \end{bmatrix} = \begin{bmatrix} 0.2516 & 0.5000 & 0.2484 \\ 0 & 2.7802 & 5.5604 \end{bmatrix}$$

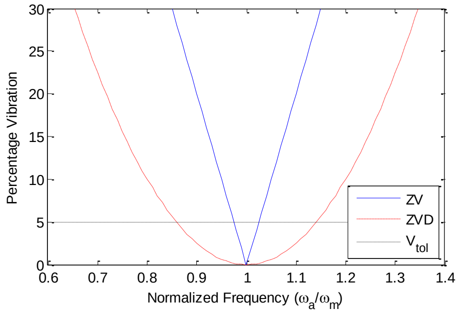

Fig. 8: The insensitivity curve of ZV and ZVD

Similarly, the ZVD shaper can also be designed robust to the damping ratio. However, it is unnecessary for our model. When $\xi = 0.01$ (i.e. expands to 500% of 0.002), the rate of change of K is just (0.9937-0.9691) /0.9937 = 2.48%, which can hardly change the values of A_i and t_i. So the ZVD shaper is robust to the change of the damping ratio because ξ is too small.

There is a conflict between robustness and rapidity. When an impulse is added, the settling time increases by half of the oscillation period. Theoretically, ZV is faster than ZVD while ZVD is more robust than ZV. For the FAST cable-cabin system, its natural frequency is variable due to the flexible structure, which means the planning algorithm requires more robustness. When it comes to the settling time, ZVD costs about more 2.78 seconds than ZV does, which is not significant in the slewing task. Although there are many other shapers that are more robust than ZVD, such as Extra-Insensitive shaper and Specified-Insensitivity shaper, they cost much more time than ZVD. ZVD reaches a satisfying compromise between robustness and rapidity.

4 Simulation and Analysis

Based on the description of the cable-cabin model and the cascade trajectory planning algorithm in Section 2 and Section 3, simulation experiments are set up with Simulink blocks. In this section, two experiments will be conducted: (1) For the slewing task, compare and analyze the vibration under s-curve planning and cascade trajectory planning; (2) Test the robustness of the cascade trajectory planning.

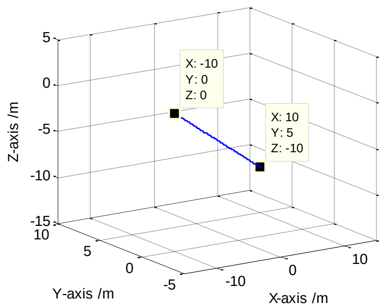

Fig. 9: The slewing task

4.1 Comparison of Different Methods in Vibration Suppression

In the slewing task, the start point and end point in the world Cartesian coordinate are (-10, 0, 0) and (10, 5, -10), the unit of distance is meter, the simulation time is set 80 seconds. All parameters of the model and planning algorithms are assigned with values discussed in Section 2 and 3.

The experiment results are shown in Fig. 10. Fig. 10 (a) (b) show the planned position profile with s-curve planning and its shaped form by ZVD (i.e. the cascade trajectory planning position profile). It is evident that the latter is smoother than the former at the cost of more settling time. Fig. 10 (c) (d) show the vibration in time domain when s-curve planning and cascade trajectory planning are applied to the model. In the process of slewing, our cascade method excites much weaker vibration than the s-curve planning does. At the 80th second, when the system is supposed to be settled, there is still residual vibration in Fig. 10 (c). Fig. 10 (e) (f) are the results of FFT analysis of (c) (d) in the frequency domain. It is evident that cascade method suppresses vibration near the natural frequency more significantly than s-curve planning does. Compared to no planning (as shown in Fig. 6), the two planning methods reduce much more vibration. Fig. 10 (g) (h) illustrate that the acceleration curve of cascade method is smoother than that of s-curve, which also accounts for the results of vibration suppression. On the other hand, the acceleration curve shows that cascade method requires more time to make the system settle down. Luckily, the cost of time is not large for slewing, given the fact that there is still some residual vibration when the cable-cabin system is supposed to be settled with s-curve planning.

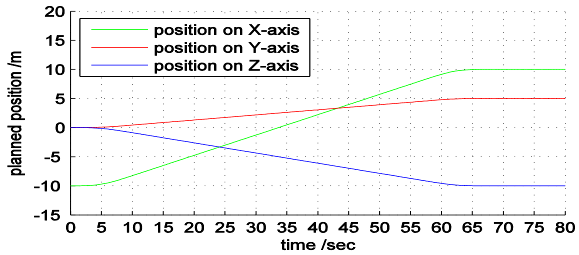

(a)

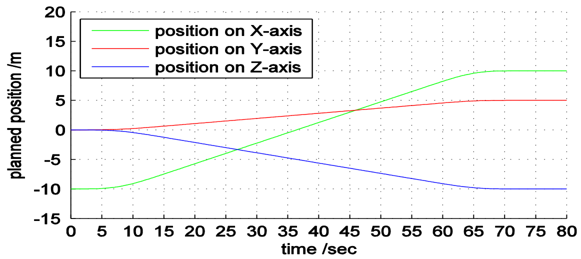

(b)

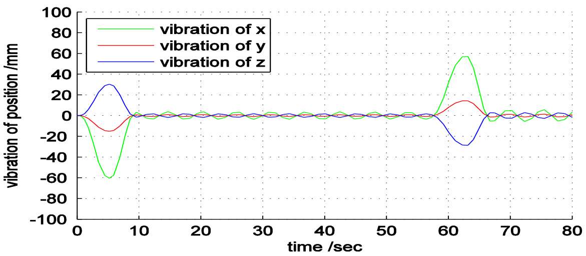

(c)

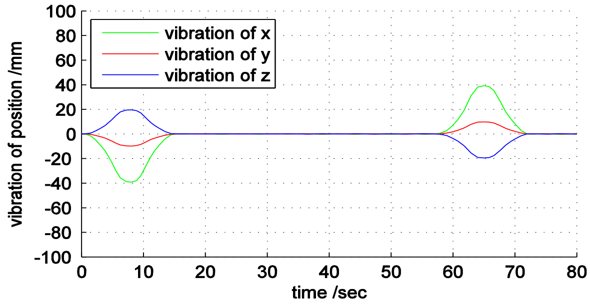

(d)

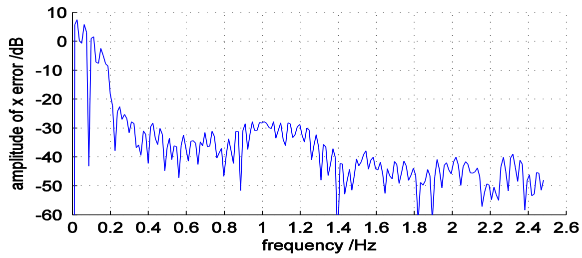

(e)

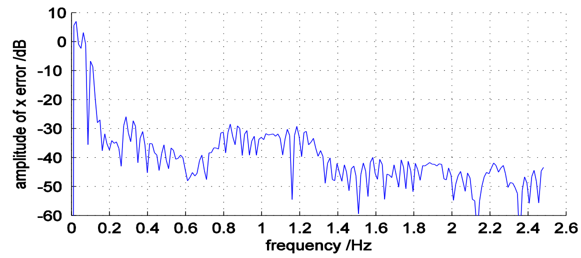

(f)

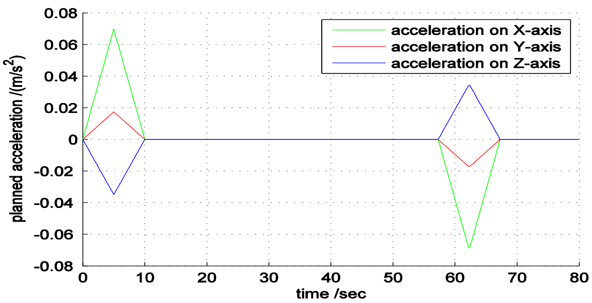

(g)

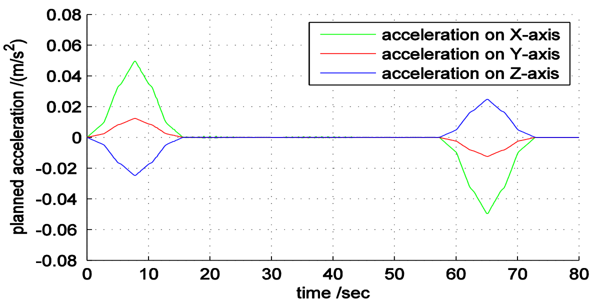

(h)

Fig. 10: Comparison of s-curve planning and cascade planning

4.2 Test of Robustness

As mentioned in Section 2, the cable-cabin system of FAST vibrates at a set of multiple frequencies. Due to the flexibility, the main natural frequency will vary in some range. It is necessary to test the robustness of the cascade method. The ZVD shaper in the cascade trajectory planning algorithm is designed with $f_n = 0.18,\ \xi = 0.002$. Then the algorithm is tested with the real natural frequency $f_n = 0.14$ and 0.22. Fig. 11 shows that when the real natural frequency floats around the nominal one with limited deviation, the residual vibration after the settling time is still not significant. The results illustrate that the cascade trajectory planning is robust to the change of natural frequency.

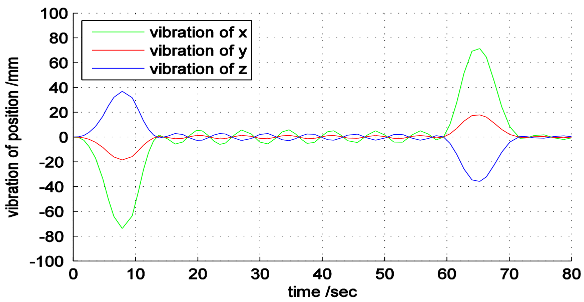

(a)

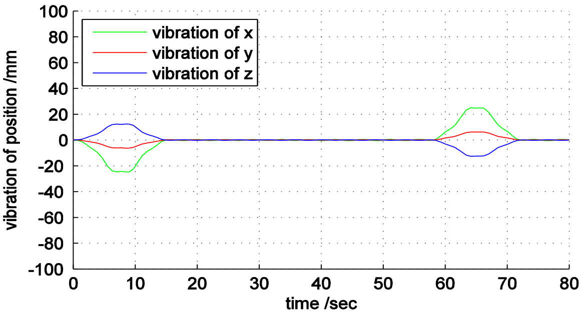

(b)

Fig. 11: Vibration under different real natural frequencies with the same shaper, (a) $f_n = 0.14$, (b) $f_n = 0.22$

5 Conclusion and Future Work

To alleviate the vibration of the focus cabin excited by the acceleration and deceleration during slewing, the cascade trajectory planning is proposed. Based on a simplified model, the simulation experiments are conducted. The results prove that the cascade method is more effective than s-curve planning in vibration suppression during slewing. Tests with various real natural frequencies illustrate cascade method's robustness to the change of the natural frequency. However, the real system vibrates at a set of multiple frequencies, so in the following research, the method should be designed to adapt to multi-mode vibration. What's more, whether the proposed method could be modified to suppress vibration in other tasks besides slewing, such as tracking and self-defined scanning, still requires more research.

References

[1] Nan R D, Five hundred meter aperture spherical radio telescope (FAST), *Science in China series G Physics, Mechanics & Astronomy*, 49(2): 129-148, 2006.

[2] Deng S, Jing F S, Yang G D, et al. Research on trajectory planning of On-The-Fly observing for the active feed receiver in FAST, *Chinese Control Conference. IEEE*, 2015: 4393-4399.

[3] Sun J H, Zhu W B, Nan R D. Design of reaction mass dampers in the suspension for the FAST focus cabin, *Astronomical Research & Technology*, 6(1): 36-42, 2009.

[4] Su Y X, Duan B Y, Wei Q, et al. The wind-induced vibration control of feed supporting system for large spherical radio telescope using electrorheological damper, *Chinese Journal of Mechanical Engineering*, 13(2):95-110, 2001.

[5] Su Y X, Duan B Y, Nan R D, et al. Application of electrorheological fluids in semi-active wind vibration control of the feed supporting system for the large radio telescope, *Jounal of Xidian University*, 28(2):163-167, 2001.

[6] Dong Z D B Q Y. Dynamical analysis of cabin of the large telescope under wind and MTMD damper designed, *Chinese Journal of Applied Mechanics*, 19(3):116-119, 2002.

[7] Wei Q, Qiu Y, Duan B. Vibration control of the suspended feed cabin structure of the large radio telescope, *Journal of Vibration & Shock*, 2001.

[8] Zi B, Duan B Y, Du J L, et al. Modeling and active control of a cable-suspended parallel manipulator, *Journal of Vibration & Shock*, 26(3):96-100, 2007.

[9] Singhose W. Command shaping for flexible systems: A review of the first 50 years, *International Journal of Precision Engineering and Manufacturing*, 10(4):153-168, 2009.

[10] Smith, O. J. M., Posicast control of damped oscillatory systems, *Proceedings of the IRE*, 45(9): 1249-1255, 1957

[11] Singer, N. C. and Seering, W. P., Preshaping command inputs to reduce system vibration, *Journal of Dynamic Systems, Measurement & Control*, 112(1): 76-82, 1990.

[12] Singhose, W. E., Seering, W. P. and Singer, N. C., Shaping Inputs to Reduce Vibration: A vector diagram approach, *Proc. IEEE Int. Conf. on Robotics and Automation*, 1990: 922-927.

[13] Singhose, W., Seering, W. and Singer, N., Input shaping for vibration reduction with specified insensitivity to modeling errors, *Proc. Japan-USA Sym. on Flexible Automation*, 1996: 307-313.

[14] Kärcher H J, Li H, Sun J, et al. Proposed design concepts of the FAST focus cabin suspension, *SPIE Astronomical Telescopes + Instrumentation, International Society for Optics and Photonics*, 2008:701239-701239-9.

[15] Berardinis L A. Motion control gets gradually better, *Machine Design*, 1994.

[16] Meckl P H. Optimized s-curve motion profiles for minimum residual vibration, *Proceedings of American Control Conference*, 1998:2627-2631.